9

Zimm-Bragg Model Applied to Sorption of Dyes by Biopolymers: Alginic Acid and Xanthan

Juan Jáuregui-Rincón,
Juan Antonio Lozano-Alvarez and Iliana Medina-Ramírez
Universidad Autonoma de Aguascalientes,
Mexico

1. Introduction

Dyes and dyeing processes are widely used as a means of introducing color into fibers or fabrics. Dyes should be easily introduced into the fiber and then, the color must be reasonably permanent (wash-fast) and stable to light (light-fast). Dyes exhibit considerable structural diversity and are classified by their chemical structure, application to the fiber type and/or solubility. A general classification accommodates these compounds as anionic (acid, direct and reactive dyes); cationic (basic dyes); and non ionic (disperse dyes). Disperse Yellow 54 (DY54) is a typical dye which can be used in dispersed form to color polyester, polyamides, nylon, acrylic fibers and plastics. Direct Black 22 (DB22) is a cationic compound (at neutral pH) that imparts color to cotton, cellulose, leather, wool and silk (Holme, 2000; Alí, 2005). The chemical structures of DY54 and DB22 are represented in table 1.

Despite the fact that supercritical methods (Ozcan et al., 1997; Joung & Yoo, 1998; Guzel and Akgerman, 1999; Lee et al., 1999; Sung & Shim, 1999; Shinoda and Tamura, 2003; Hou & Dai, 2005) have been developed to improve the performance of dyeing processes, still conventional (dye baths) methods are widely used (Holme, 2000). During dyeing processes great amounts of unfixed dyes (which vary considerably depending on dye-fiber affinity and dyeing process parameters) may be lost to the effluent. The release of these effluents in water streams results in serious environmental impacts. The development of an environmentally benign methodology for the removal of dyes from textile wastewaters still represents a major technological challenge. It is well known that textile industries, pulp mills and dyestuff manufacturing discharge highly colored wastewaters which represent an aesthetic problem and reduce photosynthetic activity in the receiving water into which they are discharged. Nowadays, many dyes are designed for their chemical stability (wash and light fastness) and do not undergo biochemical degradation readily. For instance, anthraquinone based dyes are more resistant to biodegradation (oxidation rates are very slow) due to their fused aromatic structures (Baughman & Weber, 1994). Since azo dyes are the most widely used, several degradation methods have been implemented to remove them from water, among them, anaerobic treatments predominate. The main drawbacks of this approach are its elevated cost and the production of carcinogenic aromatic amines which limits macro-scale application (Ogawa & Yatome, 1990; Knapp & Newby, 1995; Weber & Adams, 1995).

Dye	Structure
Disperse Yellow 54 (DY54)	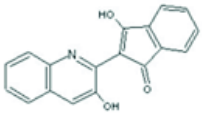
Direct Black 22 (DB22)	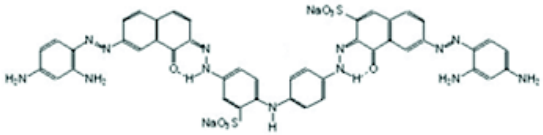

Table 1. Structure of disperse Yellow 54 (DY54) and Direct Black 22 (DB22).

Adsorption has been observed to be an effective process for color removal from dye wastewater. Use of activated carbon (powdered, nanotubes and chemically modified) has been found to be effective, however, the cost of this adsorbent has led to the search for new, less expensive alternatives for the treatment of polluted waters (Choy et al., 2000, 2004; Mittal, 1996; Fugetsu et al., 2004). Recently, numerous studies have focused on biomaterials (wood sawdust, lichens, plant residues and biopolymers) that are capable to remove dyes from wastewaters (Chakraborty et al., 2006; Poots & McKay, 1976; Sun & Xu, 1997; McKay et al., 1982, 2003; Trung et al., 2003; Gibbs et al., 2004; Wong et al., 2004; Hu et al., 2006). In a recent report, several polysaccharides (chitin, chitosan, locust bean gum, guar gum, corn starch, wheat starch, pectin, carrageenan, dextrin, alginic acid, tamarind gum and cassia gum) were evaluated as adsorbents to remove color from synthetic dyeing effluents. Elevated degrees of color removal were encountered for chitosan (94%), Locust bean gum (85%) and cassia gum (81%) (Blackburn, 2004). Although the study remarks the sorption capacities of the biopolymers, kinetic and equilibrium sorption parameters were not described.

The adsorption behavior of modified alginate (MA) was studied toward the removal of basic dyes (Nasr et al., 2006). The equilibrium time for the adsorption process was found to be 70 min. Electrostatic interactions between the dyes and the adsorbent govern the adsorption mechanism. The results revealed that the adsorption of basic dyes onto MA fit well with both Freundlich and Langmiur isotherms. To our knowledge, the sorption capability of xanthan for the removal of dyes has never been evaluated. In this work we report the sorption capacities of alginic acid and xanthan for the removal of DY54 and DB22. Mathematical models were applied in order to elucidate the adsorption mechanism of the biopolymers and process variables were optimized.

1.1 Alginic acid

Alginic acid is an anionic polysaccharide which consists of long chains of β(1→4)-linked homopolymeric β-D-mannuronate (M) blocks and linear chains of α(1→4)-linked α-L-guluronate (G) residues. The conformation of alginic acid varies, thus, homopolymeric blocks of consecutive G or M-residues (poly G and poly M, respectively) and heteropolymeric blocks of alternating M and G (M-G-M-G-M) chains can be encountered

depending upon the source of extraction of this polymer. This saccharide is mainly produced by brown algae and bacteria (*Azotobacter vinelandii*).
Sodium alginate absorbs water quickly, which makes it useful as an additive (gelling and thickening agent) in the food industry and in the manufacture of paper, dyestuffs and textiles. Due to calcium alginate´s biocompatibility it is widely used in different types of medical products (tablets, syrups, creams, etc.) for cell immobilization and appetite suppressant. (Lee et al., 2003).
It has been shown that the physical properties of alginates depend on the relative proportion of the three types of blocks. Alginates with a high proportion of G blocks produce rigid gels that form fairly quickly as calcium ion concentration increases. The opposite holds for alginates with mainly M blocks; the gels form gradually and are softer and more elastic. The early hypotheses for gel formation was that calcium ions displaced hydrogen ions on the carboxylic acid groups of adjacent chains and formed simple ionic bridges between the chains. Rees (1969) argued why that was unlikely and later he put forward the "egg-box model" (Grant et al., 1973), now generally accepted. In this model, pairs of helical chains are packed with the calcium ions located between them (Glazer & Nikaido, 1995; Siew & Williams, 2005). Initially it was believed that the G chains were the only ones responsible for Ca^{+2}-Alginate gel formation since the distances between carboxyl and hydroxyl groups are ideal for Ca^{+2} packing. Recently Donati et al. (2005) suggested that not only G blocks but also random GM blocks contribute to the Ca^{+2}-alginate interaction.
Whereas the monovalent cation (Na^+, K^+, NH_4^+) salts of alginic acid, are soluble in water, alginic acid and calcium alginate are not; therefore, this property can be exploited for the simple removal of alginate from solution. Alginates are more stable in the pH range of 5-9 ($pK_{a(M)} = 3.38$, $pK_{a(G)} = 3.65$) (Maurstad et al; 2003; Hughet et al; 1994). Below pH 5, the free carboxilate ions in the polymer chains start to become protonated, therefore, the electrostatic repulsion between chains is reduced and the proximity of the chains promotes hydrogen bond formation, producing higher viscosities. If the pH is quickly reduced from 6 to 2, a gelatinous precipitate of alginic acid will form.
In this work, we employed alginic acid as adsorbent to remove dyes from aqueous solution. The complex alginate-dye was easily removed from solution upon addition of Ca^{+2} ions or lowering the pH of the solution.

1.2 Xanthan

Xanthan is an exopolysaccharide produced by the bacterium *Xanthomonas campestris*. Due to its unique rheological properties (high viscosity, tolerance to a wide range of temperature, pH and salt concentration) it is widely used in the food industry as thickening, stabilizing or suspending agent. The chemical structure of xanthan has been elucidated. It is an acidic polymer made up of pentasaccharide subunits, forming a cellulose backbone with trisaccharide side-chains composed of mannose β(1→4)glucuronic-acid β(1→2)mannose attached to alternate glucose residues in the backbone by α(1→3) linkages (Jansson et al., 1975). On approximately half of the terminal mannose residues a pyruvic acid moiety is joined by a ketal linkage. Acetyl groups are often present as 6-*O* substituents on the internal mannose residues. Some external mannoses contain a second 6-*O*-acetyl substituent. The degree of pyruvate substitution depends on the fermentation process and on the strain of xanthomonas bacteria. (Glazer & Nikaido, 1995; Goodall & Norton, 1987).
In the solid state, xanthan gum is a two-stranded polymer that presents a highly symmetric helix conformation. The two antiparallel polysaccharide strands wind in a right-handed

manner (Glazer &Nikaido, 1995; Goodall & Norton, 1987). A significant feature of this structure is that the trisaccharide side chains are arranged close to (and hydrogen bonded to) the glucan backbone, which could be expected to stabilize a stiff helical conformation in solution. In aqueous solutions, the average molecular weight of xanthan (single helix) ranges from 2 to 15 megadaltons (MDa). The substituents (pyruvil and acetyl groups) play a moderate role on conformational stability and rheology of xanthan in solution (Rinaudo, 2004). Conformational transition (helix-coil transition) is often observed to be dependent on solution conditions. A mixture of single and double helical conformation predominates in the presence of concentrated salt solutions.

Rod et al. (2001a; 2001b) reported that in the presence of trivalent ions, in particular, aluminum ion, xanthan solutions form a semireversible gel that sets with the addition of heat. The aluminum ion favors intermolecular associations of xanthan gum which renders a marked reduced solubility and ease of separation of the polymer from solution. In this work we utilized this approach to separate the xanthan-dye complex once the adsorption process was terminated.

1.3 Zimm Bragg model

Adsorption is often described in terms of isotherms, which show the relationship between the bulk aqueous phase activity (concentration) of adsorbate and the amount adsorbed at constant temperature. One of the initial models for the adsorption of a species onto a simple surface was put forth by Irving Langmuir in 1916. Langmuir assumed that a surface consists of a given number of equivalent sites where a species can physically or chemically stick. It is important to realize that the processes of adsorption and the opposite process (desorption) is dynamic; a rate law can be written for each process, and when the rates become equal an equilibrium state will exist characterized by a constant fractional coverage of the original sites. Motivated by the dependence structure-function of biomolecules, conformational transitions in biopolymers have been a subject of extensive research; especially, since these conformational transitions can be induced (or manipulated) by a variety of stimuli (temperature, pH and ionic concentration). The coil to helix transition of polymers in solutions is a common and very important phenomenon that affects the adsorption capabilities of these biomolecules. This transition occurs from a randomly coiled conformation with considerable freedom of reorientation around the bonded repeating units to a helix conformation, characterized by bond rotational angles that are fixed within very narrow limits. The cooperative nature of conformational transitions of polypeptides has been understood for three decades through the theoretical work of Zimm and Bragg and later refinements, however, an explanation for the range of conformations possible in polysaccharides and the principles governing intramolecular interactions are less well understood (Zimm & Bragg, 1959). The polydispersity of polymers results in competing adsorption of the thermodynamically favored larger molecules for surface sites filled initially by smaller molecules. Different segments of a block copolymer may exhibit quite different adsorption characteristics, complicating the rearrangement process further. Despite the difficulties encountered in polymers behavior, predictions of conformational enthalpy and heat capacity have been reported using the Zimm-Bragg theory (Kromhout, 2001).

Pioneering work on the application of Zimm-Bragg theory to polysaccharide-surfactant systems was conducted by Satake & Yang (1976). The features of interaction between surfactant and polymer can be represented on binding isotherms. One of the binding features is the cooperative nature of interaction. The cooperativity of the binding is taken

into account by an additional cooperativity factor, and the Zimm-Bragg model is then applied to the array of occupied and unoccupied sites.
Binding isotherms can be constructed by plotting β (binding coefficient, defined as fraction polymer sites occupied by an exogenous molecule (i.e. surfactant, dye) divided by total potential sites of binding) versus log Ce (surfactant concentration at equilibrium) resulting on a sigmoid curve. From this, it was concluded that not only electrostatic interactions govern adsorption of hydrophobic molecules (such as surfactants) to polymers, but also hydrophobic interactions (micelle formation) contribute to the sorption process. It was proposed that two processes are responsible for aggregate formation: Nucleation and aggregation. Nucleation is the process in which one surfactant molecule binds to a site adjacent to a site already occupied by other surfactant molecule; this step is determined by the magnitude of K_u, and is represented by the following equation:

$$K_u = \frac{(DD)}{(ED)(D)} \tag{1}$$

Where DD denotes two adjacent sites occupied by two surfactant molecules and E indicates an empty site in the polymer. The cooperativity parameter u, is defined as:

$$u = \frac{(DD)(EE)}{(DE)^2} \tag{2}$$

The equation that correlates β with K_u is as follows:

$$\beta = \frac{1}{2}\left\{1 - \frac{(1-s)}{\sqrt{(1-s)^2+\frac{4s}{u}}}\right\} \tag{3}$$

Where s represents Ku C_e. The other parameters are defined as

$$[k_u]^{-1} = \left[C_{e(\beta=0.5)}\right] \tag{4}$$

and

$$\frac{d\beta}{d\log C_{e(\beta=0.5)}} = \frac{\sqrt{u}}{4} \tag{5}$$

Optimization processes can be applied in order to determine the best values of u and K_u that describe the polypeptide-surfactant system. Although there are numerous reports regarding interaction of polypeptides to surfactants, few works have been published related to polymer-surfactant interactions. Polymer-surfactant interactions can be divided into two classes: binding to neutral polymers and to polyelectrolytes (Liu et al., 1997). In the latter case, polyelectrolytes are viewed as a one dimensional array of binding sites that bind ionic surfactant ions with opposite electric charge. In the present study we will describe the interaction of dyes (DY54 and DB22) to the biopolymers, alginate and xanthate.

2. Experimental procedures

2.1 Optimization of adsorption conditions

2.1.1 Dye purification

In order to elucidate the adsorption mechanism of dye-polymer, dye additives (dispersing agent, salts, binder, etc.) were removed. A solution of the commercial dye was prepared and cleaned trough a silica column. The purity of the dyes was evaluated by HPLC.

2.1.2 pH optimization

Samples of 500 mg of biopolymer (sodium alginate or sodium xanthan) were placed in a flask, and 50 ml of distilled water were added. The mixture stood for a period of 5 h to facilitate hydration. 40 ml of dye solution (250 ppm) were added. The pH was adjusted to the desired value by the addition of acid or alkaline solution, and control of the medium ionic strength was achieved by addition of NaCl crystals. The flask was then closed and placed in a bath at 28°C, for 20 h. After the contact time period, 30 ml of jellifying agent solution ($CaCl_2$ 5% w/w, HCl 20% w/w, $AlCl_3$ 5% w/w) were added. For alginate, calcium chloride and hydrochloric acid solutions were employed as jellifying agents, whereas xanthanate was treated with and without aluminum chloride. In the case when $AlCl_3$ solution was omitted, the same volume of water was added. The supernatants were separated from the solid phase by centrifugation, and the concentrations of dyes in solution were determined from the respective analytical curves. The quantity of the dyes adsorbed was determined by the following equation:

$$\%\ of\ removal = \frac{(C_i - C_e)100}{C_i} \tag{6}$$

where C_i is the initial concentration of dye in solution (mgL^{-1}), and C_e is the final concentration of dye in solution (mgL^{-1}).

2.2 Adsorption isotherms

The adsorption isotherms were obtained by the batch method, employing 500 mg of biopolymer and 50 mL of the dye solution at different concentrations (5-2000 ppm). The dye solutions were prepared at a pH and ionic strength values, optimal for adsorption. These solutions were stirred until they reached adsorption equilibrium (20 h at 28°C). The complex dye-polymer was separated and the quantity of dye adsorbed was determined by employing a UV-Vis spectrophotometer, Thermospectronic model Genesys, in the respective λ_{max} of each dye.

2.2.1 Surfactant influence

The adsorption isotherms were obtained in the presence of different surfactants (sodium dodecyl benzenesulfonate (SDS), dodecyl trimethylammonium bromide (DTA) and Tween 80 (T80). The adsorption procedure was the same as the one indicated in previous paragraph differing only in the preparation of dye solution. In this case, different amounts of surfactants were added in order to evaluate their effects at different concentrations (0 – 100 ppm).

2.3 Adsorption models

To evaluate the applicability of Langmuir and Freundlich isotherm models, the adsorption capacities were determined and data was fitted within the model. Experimental data was analyzed via the following equation:

$$q_e = \frac{(C_i - C_e)V}{m} \tag{7}$$

Where q_e, is the amount of dye adsorbed on determined mass of the biopolymer (mol of dye adsorbed by mol of biopolymer) at equilibrium, C_i is the initial dye concentration ($molL^{-1}$), C_e, is the equilibrium dye concentration ($molL^{-1}$), V is the volume of the dye solution (L),

and ***m***, is the mass of the biopolymer (mol). There are several isotherms models available for analyzing experimental data and for describing the equilibrium of adsorption. Every model was analyzed using the software Statistica. The data was optimized against the different models.

2.4 IR and Raman analysis

IR and Raman spectroscopy were used in order to determine the functional groups involved in the dye-polymer adsorption process. The complexes dye-alginate and dye-xanthanate were washed with distilled water and dried for a period of 24 to 36 h at 60°C. The dried powders were used for the analysis. Dye-biopolymer complexes, pure dyes and pure polymers were analyzed by IR (KBr pellet) and Raman (microRaman) spectroscopy.

3. Results and discussion

3.1 UV-Vis spectroscopy

Solution behavior of DY54 was studied by UV-Vis spectroscopy. The absorption spectrum of the dye (15 ppm or $5x10^{-5}$ M solution) was found to be pH sensitive (Figure 1). Our results showed that a variation in the pH value from 11 to 11.3 produced a shift on the maximum absorption peak from λ= 376 nm to λ = 373 nm, moreover, a small hypsochromic displacement was also observed (from λ= 223 to λ = 220) when the pH was changed from 11.3 to 11.8. We do believe that the pKa values of the dye are within this range of pH, thus the shifts observed on the absorption spectrum correspond to the protonated and deprotonated forms of DY54. It is important to remark that the shifts observed on Figure 1 correspond to the influence of pH on the monomeric form of the dye since variable concentration experiments indicated that DY54 forms aggregates at concentrations higher than 100 ppm.

The absorption spectrum of DY54 exhibits a spectral blue shift as dye concentration is increased in aqueous solution. There are some reports that discuss on the formation of dye aggregates in concentrated solutions. Lai et al (1984) investigated the spectral properties of thionine in aqueous solutions at different concentrations and observed that the absorption maxima were shifted gradually and continuously to shorter wavelengths (blue shift) as the concentration of thionine was increased. In accordance to the McRae-Kasha exciton model, they attributed these observations to the formation of H aggregates (for hypsochromic). Later reports indicated that concentrated aqueous solutions of pseudoisocyanine dyes also present ordered molecular assemblies of dyes.

In contrast to the blue shift observed for thionine type dyes, cyanine aggregates exhibit a spectral shift toward longer wavelengths with respect to the monomer absorption. (Berlepsch et al., 2000). The kind of aggregates formed for cyanine dyes are called J-aggregates (named in honor of the researchers who discovered the phenomenon).

In the case of J-aggregates, the monomeric molecules are arranged in one dimension to achieve a parallel orientation of their transition moments with a zero angle between the transition moments and the line joining the molecular centers. Intermolecular interactions involving substituents on the aromatic rings act to stabilize J-aggregates.

On the other hand, H-aggregates assemble strongly coupled monomeric dye molecules in one dimension to achieve a parallel orientation of their transition moments and a perpendicular alignment of the transition moments to the line of molecular centers.

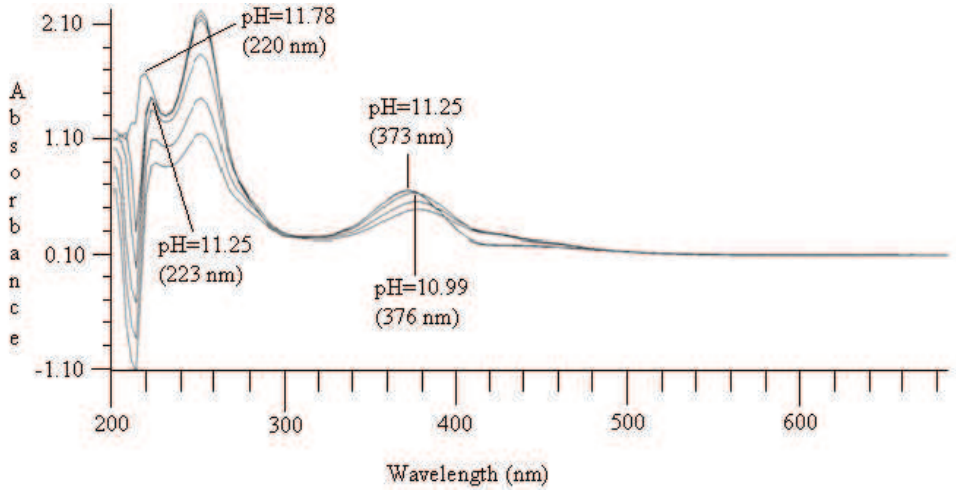

Fig. 1. UV-visible absorption spectra of DY54 (5x 10^{-5} M) in water at different pH values (with permison of J. Mex. Chem. Soc.)

The π-π interactions between aromatic rings stabilize H-aggregates. (Karukstis, 2002). The blue shift observed in the absorption spectrum of DY54 suggests the formation of H aggregates in aqueous solution.

To confirm our hypothesis of dye aggregates formation, the absorption spectrum of DY54 was evaluated at different temperatures. It is well known that increasing temperature will increase the dissociation of the dye aggregates. The absorption spectra of DY54 at the temperatures of 20, 30, 50, 60 and 80°C are given in figure 2.

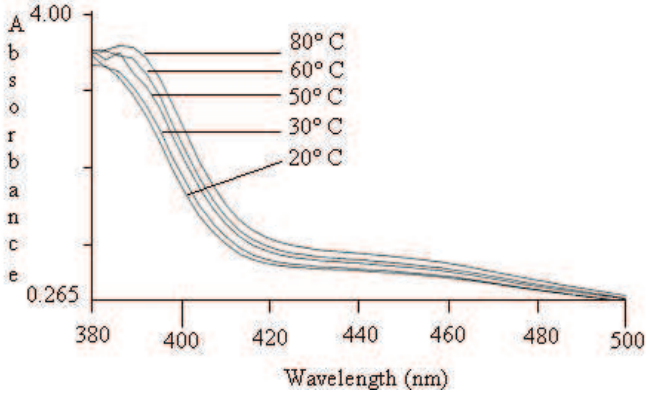

Fig. 2. UV-visible absorption spectra of DY54 (125 ppm) in aqueous solution at different temperatures

We observed that as temperature was raised, the absorption maxima shift gradually to longer wavelengths; from here we concluded that concentrated solutions of DY54 form H aggregates that dissociate into smaller aggregates which explain the red-shifted band.

In this work we also investigated the interactions of DY54 with polymers (ALG and XANT) and jellifying agents ($CaCl_2$ and $AlCl_3$) in solution by UV-Vis spectroscopy. It has been reported that the interaction between cationic dyes with anionic polymers alter the absorption spectrum of the dyes. The polymers induce metachromasy in the dye as evidenced from the considerable blue shift in the absorption maxima of the corresponding dyes. Mandal (1990) and collaborators studied the interaction between the dyes (1,9-dimethylmethyleneblue and pinacyanol) and alginate by UV-Vis spectroscopy. It was observed that alginate induce metachromasy in the absorption spectrum of 1,9-dimethylmethylenblue and pinacyanol. In our work, different amounts of alginate solution were added to a 15 ppm DY54 aqueous solution and the readings were taken after at least half an hour of mixing. From our spectra, it can be observed that DY54 does not exhibit metachromasy in the presence of polymers (ALG and XANT).
Aluminum chloride was used as precipitating agent for the DY54-XANT complex. The interaction between DY54 and $AlCl_3$ was evaluated by UV-Vis spectroscopy. As observed for DY54-ALG, the absorption spectrum of DY54 does not alter its position nor its shape after addition of small aliquots of $AlCl_3$ solution, however, after addition of 20 mL of $AlCl_3$ solution, the pH of the solution was changed (from 11.8 to 11.3) inducing DY54 protonation which is responsible of the shift observed for the absorption spectrum of the dye under this conditions.

3.2 Sorption studies

3.2.1 ALG-DY54 (HCl) system

To optimize the adsorption process different variables were evaluated. The concentration of the dye solution was kept constant at 50 ppm. Figure 3 illustrates the effect of pH and ionic strength (I) on dye removal. From the graph, we can see that ionic strength does not affect considerably adsorption process however as pH decreases the amount of dye removed is considerably increased. The pH value could not be further decreased since precipitation of alginate occurs below this value. From this figure 3 we can easily conclude that maximum adsorption (83%) can be pursued when the pH value is 10.8 and I = 0.9M. These observations indicate that at elevated pH values both molecules (dye and polymer) are negatively charged thus electrostatic repulsion minimizes the interaction dye-polymer whereas at lower pH values the formation of neutral molecules facilitates this interaction. Increasing the ionic strength of the solution produces the "salting out" effect, thus, dye molecules tend to agglomerate. Dye agglomerates adsorb more easily to the polymer than the monomeric more soluble form of the dye.

3.2.2 XANT-DY54 system

The removal of DY54 by xanthan was explored. The effect of pH and ionic strength was evaluated. Results are illustrated on Figure 4. Adsorption maxima was achieved at a pH value of 11.3 and ionic strength of 0.9M. Under these conditions a removal efficiency of 96% (using a DY54 50 ppm solution) was accomplished. As discussed for ALG-DY54 system, micelle-like clusters adsorbed to the polymer chain are also believed to represent the binding in this case. This would suggest that adsorption of DY54 onto xanthan and alginate occurs through a combination of hydrogen bonding and hydrofobic interactions.

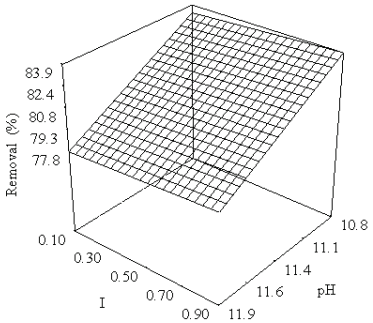

Fig. 3. Removal of DY54 by alginic acid as function of pH and ionic strength. (with permission of J. Mex. Chem. Soc.)

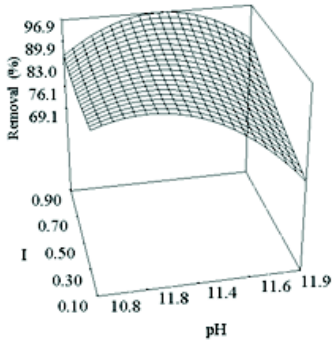

Fig. 4. Removal of DY54 by xanthan as function of pH and ionic strength. (with permission of J. Mex. Chem. Soc.)

3.2.3 ALG-DY54 ($CaCl_2$) system

Our results indicate that the use of $CaCl_2$ as jellifying agent (JA) contributes to increase the DY54 (50 ppm) removal efficiency of the polymer from 83% (using HCl as JA) to 90% (see figure 5).

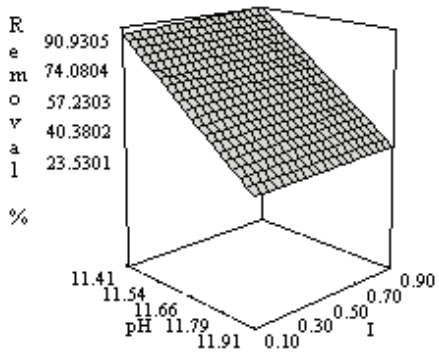

Fig. 5. Removal of DY54 as function of pH and ionic strength by alginic jelled with calcium chloride.

The adsorption capacity of biopolymers depends on their physical structural parameters such as crystallinity, surface area, porosity, particle type, particle size and water content. Alginate hydrogels consist of three dimensional, hydrophilic, polymeric networks which macromolecular conformation depend on the composition of alginate and on the JA used for gel formation. The ability to control the pore properties of the alginate gels is difficult due to rapid gelation mechanism. We observed an increased capacity for dye adsorption of ALG($CaCl_2$) compared to ALG(HCl). This observation may have different justifications since the pore size and pore properties of the gels are different. Despite the fact that acid gels are more flexible that Ca-ALG gels, it is possible that the pore size is smaller impeding dye molecules (aggregates) diffuse freely into the gel. In the case of Ca-ALG besides the amount of dye adsorbed on the surface, there is the possibility that the gel is able to encapsulate dye aggregates within its network, increasing the adsorption capacity of the gel.

3.2.4 XANT-DY54 (Al) system

The addition of aluminum chloride as gelling agent to XANT-DY54 system increased in notable way the removal of DY54 (figure 6).

The polymeric network formed by the interaction between Al^{3+} and xanthan molecule favors the adsorption of DY54 molecules. Rod et al (2001 a; 2001 b) proposed that the carboxilate group of the glucuronic moiety of xanthan molecule interacts with aluminum ion promoting an increase in the size of the "cluster". We do believe that the elevated adsorption shown for XANT(Al) is the result of two independent processes, first, the cavities within the XANT(Al) cluster are big enough to entrap dye molecules in their interior; and second, aluminum ion decreases the negative charge on the XANT molecule favoring interaction with dye molecules.

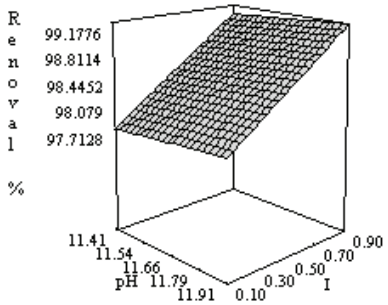

Fig. 6. Removal of DY54 as function of pH and ionic strength by alginic jelled with aluminum chloride in the system Xant-DY54 (Al).

3.3 Adsorption isotherms

Adsorption isotherms are an equilibrium expression for the amount of adsorbed solute (S) versus the solute concentration in solution (C). They can conveniently be used to describe how pollutants interact with adsorbent materials and are very important for optimization of adsorption systems. There are several isotherm models available for analyzing experimental data and for describing the equilibrium of adsorption.

An isotherm can be constructed by plotting q_e versus C_e, where q_e , represents the amount of dye adsorbed on the adsorbent material (in this particular work, biopolymers) at

equilibrium; and C_e is the equilibrium concentration of dye solution (mg/L or mol/L) . The units of q_e can be expressed as mass of dye (mg)/ mass of adsorbent (g) or as mol of dye/mol of adsorbent.

3.3.1 Langmuir isotherm

The model assumes uniform energies of adsorption onto the surface of the adsorbent with no transmigration of adsorption of adsorbate molecules in the plane of the surface. The Langmuir model assumes that adsorption takes place at specific homogeneous sites within the adsorbent, resulting on the formation of a sorbate monolayer on the sorbent surface. The linear form of Langmuir isotherm is given by the following equation:

$$\frac{C_e}{q_e} = \frac{a_L C_e}{K_L} + \frac{1}{K_L} \tag{8}$$

In this equation, q_e (mg/g) is defined as the mass of dye retained by unit mass of biopolymer; C_e (mg/L) is the equilibrium concentration of dye in solution, K_L and a_L are Langmuir Constants with following units (L/g) and (L/mg) respectively. If C_e / q_e is plotted versus C_e, a straight line is obtained with slope m= a_L/K_L and intercept in y axis equal to $1/K_L$.
Figure 7 show plotting of (C_e/q_e) against C_e, through which the values of a_L and K_L can be determined from the slope and the intercept, respectively. It has been shown in this figure that the adsorption of DY54 onto ALG(HCl) do not fit the Langmuir model. From here we can infer that the adsorption mechanism is more complex than a simple monolayer formation of DY54 onto ALG surface.

3.3.2 Freundlich Isotherm

The Freundlich equation has been employed to describe heterogeneous systems. The model assumes that adsorbent surface sites have a spectrum of different binding energies. The amount of adsorbed material results from the addition of the adsorption within all the sites, the monolayer formation does not limit this model. The linear form of the Freundlich isotherm is given by the following equation:

$$lnq_e = \frac{1}{n} lnC_e + lnK_f \tag{9}$$

Where q_e is the amount of dye adsorbed (mg/g) on the adsorbent. K_f (L/g) is the Freundlich constant related to the bonding energy. C_e is the dye concentration (mg/L) on solution at equilibrium, and 1/n is the heterogeneity Freundlich factor. The Freundlich isotherm for ALG-DY54 (HCl) is presented in Figure 8.

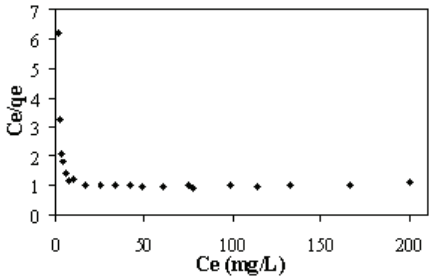

Fig. 7. Plot of C_e/q_e versus C_e to ALG-DY54 (HCl) system. (with permission of J. Mex. Chem. Soc.)

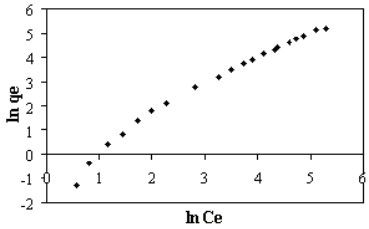

Fig. 8. Plot of lnqe versus ln Ce to obtain Freundlich parameters (K_F and 1/n parameters) in system ALG-DY54 (HCl). (with permission of J. Mex. Chem. Soc.)

The values of the Freundlich constants together with the correlation coefficient are presented in table 2.

System / Model	ALG-DY54 (HCl)		
	Parameter values	**Average error**	**R^2**
Langmuir	K_L=0.3755 a_L=-0.003449	48.13 %	0.7445
Freundlich	K_F=0.2346 n=0.7564	26.11 %	0.8694
Zimm-Bragg	Ku=3000 U=4	16.6 %	0.9878

Table 2. Sorption parameters for ALG-DY54 (HCl) system.

The Freundlich equation predicts that the dye concentration on the adsorbent will increase so long as there is an increase in the dye concentration in the liquid. Based on the correlation coefficient (0.8694) and the shape of the isotherm, it was concluded that neither Langmuir nor Freundlich models were appropriate to fit the experimental data. Despite the fact of a more complex interaction (heterogeneous surface, sorbate-sorbate interactions, sorbate migration and absorption into the pores of adsorbent) between sorbate-adsorbate considered by Freundlich model, our results do not fit accurately with this empirical model, suggesting a different mechanism of adsorption.

3.3.3 Zimm-Bragg model

Binding of surfactants to polymers is observed to start at a rather well-defined surfactant concentration, somewhat below the critical micelle concentration (cmc). Some theoretical models have been presented for polymer-surfactant interactions, all based on the structure of micelle-like clusters bound to the polymer. An approach often used in the case of polyelectrolyte-surfactant interaction is to treat the binding of the surface as site binding to the polymer. The cooperativity of the binding is taken into account by an additional cooperativity factor, and the Zimm-Bragg model can be applied to the array of occupied and unoccupied sites.

Langmuir and Freundlich models were applied to our system, however the degree of correlation between the experimental results and the sorption models was low as summarized in the information presented on Table 2. The Zimm-Bragg model was applied to our experimental data. The isotherm for the system ALG-DY54 (HCl) is presented in figure 9 and the binding parameters tabulated on table 3. The correspondence of experimental data with Zimm-Bragg isotherm and the theoretical model is evident.

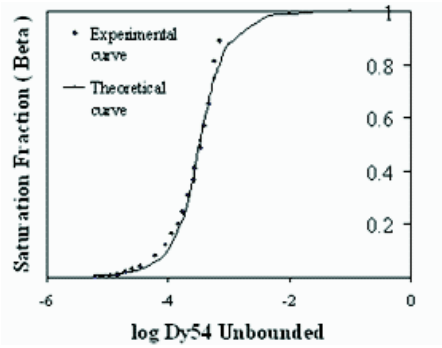

Fig. 9. Zimm-Bragg isotherm for ALG-DY54 (HCl) system. (with permission of J. Mex. Chem. Soc.)

Table 3 summarizes the binding parameters for all the dye-polymer systems [ALG-DY54 (HCl),ALG-DY54 ($CaCl_2$), XANT-DY54 and XANT-DY54 (Al)] studied in this work. A typical Zimm-Bragg isotherm is presented in figure 10 which corresponds to the XANT-DY54 system. Since our study involves a homogeneous system, the Zimm-Bragg model is the most appropriate to describe the interactions between dye-polymer.

System	Zimm Bragg Parameters*	R^2
ALG-DY54 (HCl)	Ku=3000 u=4	R^2 =0.9878
ALG-DY54 ($CaCl_2$)	Ku=685 u=200	R^2 = 0.4179
XANT-DY54	Ku=900 u=2	R^2 = 0.9811
XANT-DY54 (Al)	Ku=3100 u=200	R^2 = 0.9957

Table 3. Parameters obtained with the Zimm Bragg model in the different systems.

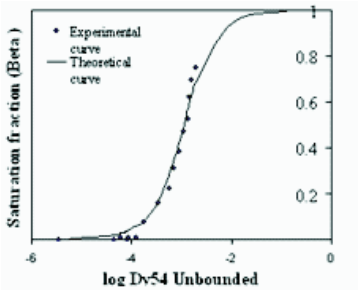

Fig. 10. Zimm-Bragg isotherm for XANT-DY54 system. (with permission of J. Mex. Chem. Soc.)

This model takes into account the formation of nucleation centers and the propagation in size to form aggregates when the dye molecules are in contact with the "molecular surface" of the biopolymer, both adsorbate (dye) and adsorbent are presents in solution and the interaction between these chemical species are always in aqueous environment. In contrast the Langmuir and Freundlich models (more specific for heterogeneous systems) consider that adsorbent is present in solid phase and adsorbate molecules are present in gas or liquid phase. In all systems where DY54 is involved all the components (DY54, biopolymers ALG

and XANT) are present as soluble species and DY54 interacts with them so that the experimental data is best described with this model.
The ALG-DY54($CaCl_2$) system presents a very low correlation coefficient value. At the working pH for this system we observed precipitation of calcium hydroxide making the solution turbid and difficult to evaluate by UV-Vis. It is possible that this system might be better described by the Freundlich model due to the presence of hydroxide salt. Currently, we are working on the elucidation of the adsorption mechanism of this system.

3.4 Infrared (IR) spectroscopy

Nuclear Magnetic Resonance (NMR) studies were conducted in order to gain a better understanding of the behavior of DY54 in solution. DY54 exists as two tautomeric forms that are illustrated on Figure 11. Our results indicate that in aqueous solution the dye adopts the keto form whereas that in the solid state (confirmed by IR) or dissolved in organic solvents, the enol tautomer conformation predominates.

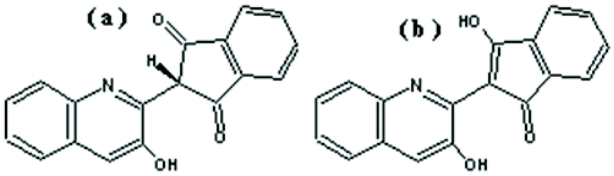

Fig. 11. Tautomeric forms of DY54: Keto (a) and enol (b).

The chemical structure of DY54, sodium alginate and ALG-DY54 (HCl) were analyzed by IR spectroscopy. The absorption spectra of the chemical species above mentioned are presented on figure 12 and a summary of absorption bands on table 4. The IR spectrum (figure 12b) of DY54 shows two main absorption bands (1656 cm^{-1} and 1547cm^{-1}) that correspond to the C=O and C=C vibrations of the DY54 enol form. The IR spectrum of ALG-DY54 (HCl) is depicted on figure 12c. The main features of the spectrum are: the absorption band at 3421 cm^{-1} that indicates hydrogen bonding among molecules (ALG-DY54) and the signal at 1736 cm^{-1} which corresponds to protonated carboxilate groups in alginate as a result of using HCl as jellifying agent.

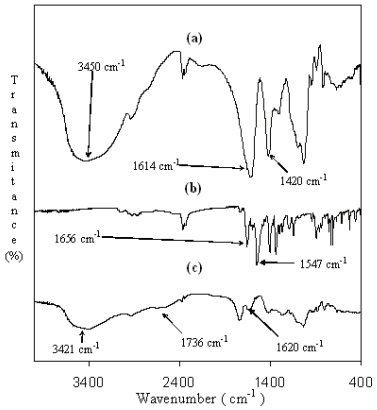

Fig. 12. FTIR spectrum of (a) alginic acid as sodium salt, (b) DY54 and (c) ALG-DY54 (HCl).

Comparison of the FT-IR spectra of DY54 and ALG-DY54 show that the principal differences among them are the shift of the C=O absorption band (1656 cm^{-1} for DY54 and 1620 cm^{-1} for ALG-DY54) and the disappearance of the peak encountered at 1547 cm^{-1} in DY54 spectrum (table 4). This suggests that keto form is the principal chemical specie that exists in ALG-DY54 (HCl) system, however one peak located at 1646 cm-1 suggests that a considerable amount of DY54 remains in the powder of ALG-DY54 as enol form. In both cases the DY54 molecules presumably can be interacting with biopolymers through hydrogen bonding.

FTIR signal	Alginate	DY54	ALG-DY54	Observations
v(O-H)	3450 cm^{-1}		3421 cm^{-1}	Hydrogen bonding between ALG-DY54
v_{as}(COO)	1614 cm^{-1}		1736 cm^{-1}	Carboxylate group protonated
v_s(COO)	1420 cm^{-1}		1420 cm^{-1}	Without changes
v(C=O)		1656 cm^{-1}	1620 cm^{-1} 1646 cm^{-1}	Hydrogen bonding where C=O of DY54 is involved. Small proportion of DY54 is encountered in enol form.
v(C=C)		1547 cm^{-1}	Disappears	Keto form of DY54 is present

Table 4. FT-IR Data of ALG-DY54 (HCl) Product.

The main IR absorption features of alginate ($CaCl_2$) gel and ALG-DY54 ($CaCl_2$) complex are tabulated on table 5. In accordance with the IR spectrum of ALG-DY54 (HCl) complex, hydrogen bonding and a shift in the carbonyl resonance (from 1656 to 1638 cm^{-1}) of DY54 are observed in the spectrum of ALG-DY54 ($CaCl_2$) complex. Torres et al. (2005) reported that the IR spectrum of calcium-alginate gels show an inversion in the intensities of the symmetric and anti-symmetric bands for the carboxilate group. Our results are in accordance with this previous report. We also observed a band at 1540 cm^{-1} that we assign to the presence of pure dye, which is present due to precipitation and lack of removal during the washing of ALG-DY54 ($CaCl_2$) complex.

FTIR Signal	Alginate ($CaCl_2$)	DY54	ALG-DY54 ($CaCl_2$)	Observations
v(O-H)	3428 cm^{-1}		3410 cm^{-1}	Hydrogen bonding between ALG-DY54
vas(COO)	1600 cm^{-1}		1600 cm^{-1}	There is an inversion in signal intensity between the two carboxylate vibrations: This signal is weaker than symmetrical vibration intensity.
vs(COO)	1408 cm^{-1}		1406 cm^{-1}	
v(C=O)		1656 cm^{-1}	1638 cm^{-1}	Carbonyl group of DY54 is involved in hydrogen bonding with alginate in presence of calcium ions.
v(C=C)		1547 cm^{-1}	1540	Still Remains traces of DY54 (enol form) in the compound ALG-DY54 ($CaCl_2$)

Table 5. FT-IR Data of ALG-DY54 ($CaCl_2$) Product.

Xanthan and XANT-DY54 complex were analyzed by IR spectroscopy. Results are presented in table 6. As expected, a resonance at 1730 cm^{-1} that correspond to the acetyl group (C=O) was observed in the xanthan's IR spectrum. As previously discussed, the formation of XANT-DY54 complex was favored at high pH values, under this condition, the acetyl group undergoes saponification, and this explains the absence of acetyl band in the IR spectrum of XANT-DY54 complex. As it was encountered for ALG-DY54 (HCl) complex, the carbonyl resonance shifts suggesting hydrogen bonding formation between dye and polymer.

FTIR signal	**Xanthan**	**DY54**	**XANT-DY54**	**Observations**
v (O-H)	3420 cm^{-1}		3381 cm^{-1}	Hydrogen bonding among XANT-DY54
v (C=O) acetyl group	1730 cm^{-1}		Very weak	Carbonyl groups in xanthan undergo saponification reaction
v_{as}(COO) pyruvate and glucuronate groups	1613 cm^{-1}		1617 cm^{-1}	Carboxylate group as sodium salt (no changes)
v_s(COO) pyruvate and glucuronate groups	1450 cm^{-1}		1450 cm^{-1}	Without changes
v(C=O)		1656 cm^{-1}	1640 cm^{-1} 1617 cm^{-1}	Some of the enol form of DY54 is present in product. Hydrogen bonding where C=O of DY54 is involved.
v(C=C)		1547 cm^{-1}	1556 cm^{-1}	Some of the enol form of DY54 is present in product.

Table 6. FT-IR Data of XANT-DY54 Product

The data from the IR analysis of XANT-DY54 (Al) are summarized in table 7. The band at 1547 cm^{-1} indicates that in the DY54-XANT complex, the DY54 is in the enol form. IR data is in accordance to Raman analysis pointing toward the formation of XANT-DY54 complexes being the dye molecule in the enol form. A proper description of the phenomenon observed is complicated due to the numerous chemical processes (such as pH modification, coagulation, interaction among aluminum ion with polymer) involved upon addition of $AlCl_3$ to the dye-polymer system.

Ethanolic solutions of ALG-DY54 (HCl), ALG-DY54 ($CaCl_2$), XANT-DY54 and XANT-DY54 (Al) complexes were prepared. For the three first examples it was observed that the solution turned yellow due to desorption of dye from the complexes. This observation supports our assumption that hydrogen bonding is responsible of dye adsorption within the polymers.

The color intensity for the alcoholic solution of complex XANT-DY54 (Al) was very weak compared to the other examples just discussed; this observation supports our proposal of the formation of cavities in the tridimensional network of XANT(Al) gel. As previously discussed we assume that these cavities are filled with dye molecules. The strength of this network cannot be broken by interaction with ethanol, thus, in solution we only observe the presence of the dye molecules that were adsorbed on the surface of XANT(Al) gel.

FTIR Signal	XANT (Al)	DY54	XANT-DY54 (Al)	Observations
v (O-H)	3421 cm^{-1}		3421 cm^{-1}	Hydrogen bonding present in XANT-DY54 (Al) complex.
v_{as}(COO) pyruvate and glucuronate groups	1629 cm^{-1}		1629 cm^{-1}	Without changes.
v_s(COO) pyruvate and glucuronate groups	1401 cm^{-1}		1401 cm^{-1}	Without changes.
v(C=O)		1656 cm^{-1}	1656 cm^{-1}	The enol form of DY54 is present in XANT-DY54 (Al) complex.
v(C=C)		1547 cm^{-1}	1547 cm^{-1}	DY54 is encountered in enol form in the product XANT-DY54 (Al)

Table 7. FT-IR Data of XANT-DY54 (Al)

3.5 Raman spectroscopy

DY54 and biopolymer-DY54 complexes were analyzed by Raman spectroscopy. The Raman spectra of DY54, ALG-DY54 (HCl), ALG-DY54 ($CaCl_2$), XANT-DY54 and XANT-DY54 (Al) are represented in Figure 13. For DY54 a characteristic absorption band at 1376 cm^{-1} (C-C=C

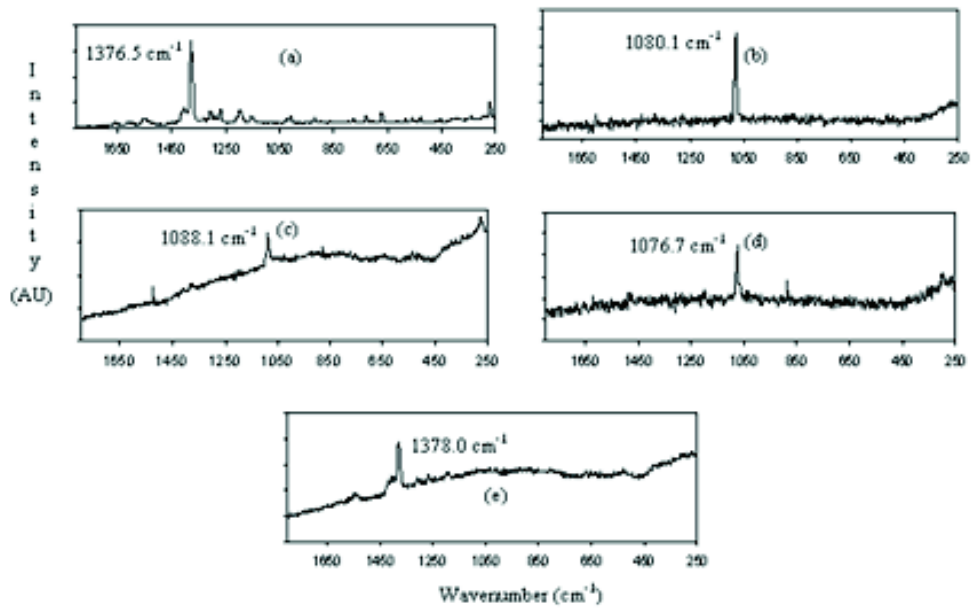

Fig. 13. Raman spectra of (a) DY54, (b) ALG-DY54 (HCl), (c)ALG-DY54 ($CaCl_2$), (d) XANT-DY54 and (e) XANT-DY54 (Al)

vibration) was encountered as the main component of Raman spectrum. The Raman spectra of ALG-DY54 (Figure 13 b and c) and XANT –DY54 (figure 13c) show a red shift (from 1378 to 1080 cm^{-1}) of the main resonance which indicates a change of the tautomeric form of the dye. As previously discussed, in the solid state, DY54 exists predominantly in the enol form upon aqueous dissolution (basic pH), the keto form predominates and is the one that binds to the polymers.
The Raman spectrum of XANT-DY54 (Al) (figure 13 e) resembles the one of pure DY54. This result confirms our assumption of different interaction are involved including electrostatic interaction between DY54 and XANT (Al). The resonance indicates that DY54 binds in the enol form. We can conclude that hydrogen bonding is the main feature of "bonding" among DY54 and ALG(HCl), ALG($CaCl_2$) and XANT, meanwhile a "mixture" of different interaction predominates in the XANT-DY54(Al) system.

3.6 Adsorption isotherms for DY54 (commercial presentation)

Since we are interested on the implementation of this process for the treatment of textile effluents, we evaluated the removal of the commercial presentation of DY54 by XANT and ALG. Our results are very similar to the ones observed for the purified form of the dye and can also be described by the Zimm-Bragg model. Interestingly, for all the systems we observed an increase in the K_u value. These results indicate that the additive(s) contained in the commercial presentation of the dye, contribute to increase the removal efficiency of the polymers.

3.7 Direct Black 22 (DB22)

3.7.1 UV-Vis spectroscopy

The solution behavior of DB22 was studied by UV-Vis spectroscopy. The absorption spectrum of DB22 was analyzed at different pH values. The spectra recorded are illustrated on Figure 14. We can see that the maximum absorption peak depends on the pH value. At a pH value of 8.35, the absorption maximum appears at 467 nm whereas that increasing the pH to 10.4 shifts the absorption maximum to 590 nm. The UV-Vis analysis for DB22 is in accordance with previous reports regarding spectroscopic studies of azo dyes in solution. The data indicate that azo dyes are affected by interactions with their environment. In our particular case, the red shift (pH related) observed for DB22 indicates a conversion of the azo form of the dye to the hydrazone and common anion forms of the dye (Abbot et al., 2004).
The formation of direct dye aggregates in solution has been reported (Monahan et al., 1970, 1971; Reeves et al., 1979; Hamada et al., 1993; Tiddy et al., 1995; Ferus-Camelo & Greaves, 2002). It was also reported that the structure of the dye determines aggregates formation (Abbot et al., 2004). The aryl groups (and the orientation of substituents) of the dye molecules facilitate the formation of aggregates via π-π stacking.

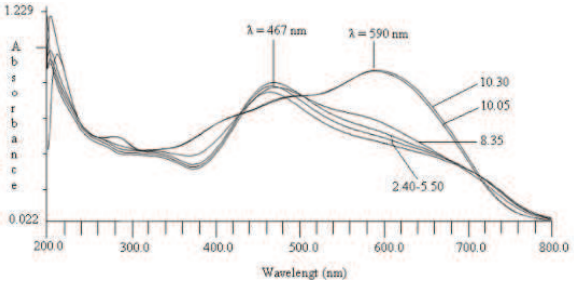

Fig. 14. UV-Visible absorption spectrum of DB22 in aqueous solution at different pH values.

Reversal of dye aggregation was analyzed by variable temperature UV-Vis spectroscopy. Spectra were recorded at different temperatures; and results are plotted on Figure 15. It is clearly shown that the absorption maximum shifts from 511 nm (20ºC) to 500 nm (80ºC) which indicates that at higher temperatures disaggregation occurs. This observation indicates the formation of "H type" aggregates by DB22.
As reported for DY54, it was observed that addition of biopolymer (alginate or xanthan) solution to DB22 solution did not affect the absorption spectrum of the dye solution.

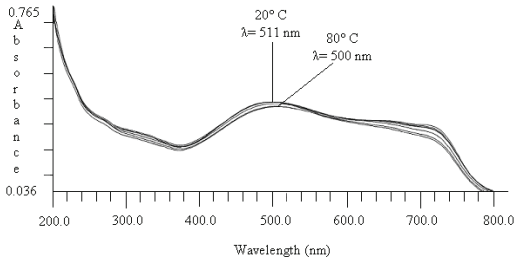

Fig. 15. UV-Visible absorption spectrum of DB22 in aqueous solution at different Temperature values (pH=4.0, ionic strength=0.1 M)

3.7.2 Surfactants influence on the adsorption isotherms for DB22 (commercial form)

Adsorption isotherms for DB22 were recorded under optimized conditions (Lozano-Alvarez et al., 2009 b). The commercial form of the dye was used in this experiment. The influence of dodecylbenzensulfonate (SDS) on the adsorption behavior of DB22 on alginate ($CaCl_2$) was evaluated. Figure 16 illustrates the adsorption isotherms for DB22 on alginate both, in the absence and in the presence of different concentrations of SDS.
The shape of the isotherm indicates that the Zimm-Bragg model describes the interaction between DB22 and alginate. We also observe that as the SDS concentration increases, the isotherm moves to the right resulting in a decrease of the K_u value. We do believe that an increase on the SDS concentration contributes to increase the dye concentration in solution diminishing the affinity for polymer adsorption.
Our results indicate that T80 at low concentrations does not form micelles and thus competes for adsorption sites against DB22, however, at elevated concentrations T80 is able to form micelles that wrap dye molecules within the core of the micelle, thus, the interaction of the dye with the polymer is two-fold, first it can bind in the form of surfactant-dye micelle and also in the form of pure dye, enhancing with this the adsorption profile (Bielska et al., 2009).
Xanthan dye adsorption was studied with and without surfactants in solution. SDS was added to a XANT-DB22 solution at different concentrations. Results are plotted in figure 17. Our results clearly show that SDS-dye interactions affect considerably the adsorption behavior of XANT(Al). Bielska et al (2009) studied the interactions of methylene blue and SDS in aqueous solution. They found that the interactions between oppositely charged dyes and surfactants are very strong, giving rise to the formation of surfactant micelles that engulf dye molecules in its interior. In our case, we studied the interaction between oppositely charged dye surfactant molecules in the presence of positively charged XANT polymer. As expected the solubility of DB22 increases due to electrostatic interactions with surfactant molecules, in the other hand, DB22 can also interact with positively charged biopolymer. Equilibrium between these two processes renders the isotherms plotted in figure 17 and indicates that surfactant-dye associations are stronger than the binding affinity toward biopolymer, thus increasing concentrations of SDS decreases the Ku for the system.

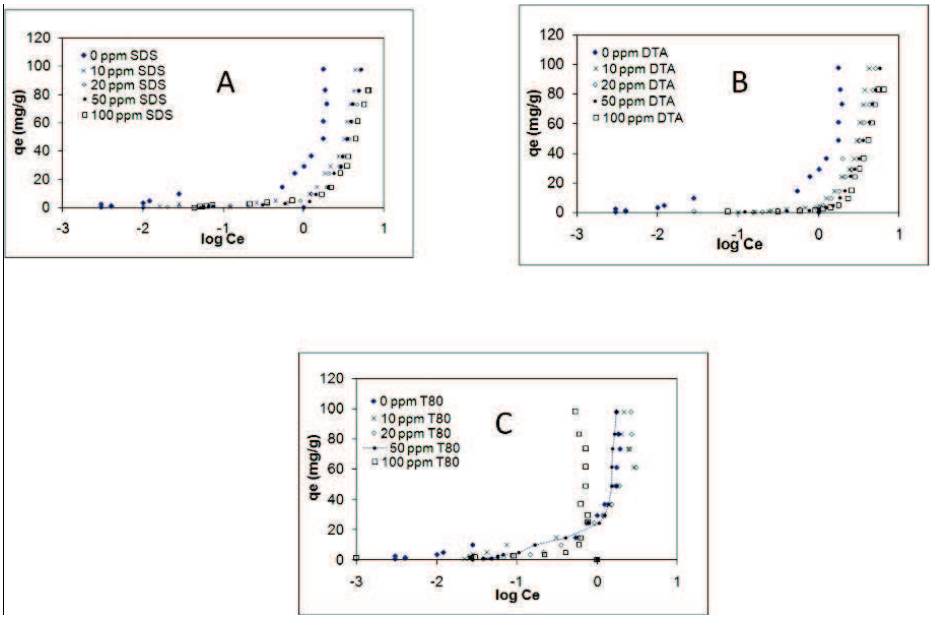

Fig. 16. Zimm-Bragg isotherms for ALG-DB22 ($CaCl_2$) with different amounts of surfactant A) SDS, B) DTA C) T 80.

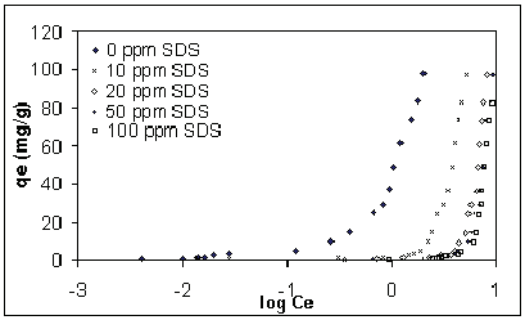

Fig. 17. Zimm-Bragg isotherms for XANT-DB22 (Al) with different amounts of surfactant SDS

The interactions between XANT(Al) and DB22 were studied in the presence of DTA. It can clearly be seen that Ku decreases as DTA concentration increases. Since both molecules (surfactant and dye) are positively charged, there is a competition for negatively charged adsorption sites on polymer. Oakes & Dixon (2003) studied the adsorption of dyes to cotton with and without surfactants in solution. It was encountered that cationic surfactants can displace adsorbed dye molecules from cotton fiber, due to higher affinity of surfactant to cotton fiber compared to dye affinity. In our particular system, XANT-DB22(DTA), we observe similar behavior, predominating DTA affinity for polymer adsorption sites. Bielska et al (2009) reported that when the same-charge dye and surfactant were used, it was found

that electrostatic repulsion forces were strong limiting surfactant-dye micelle formation. From here, we can infer that DB22 does not associate with DTA, thus interaction of DB22 with polymer is always limited for DTA interaction.

4. Conclusion

The Zimm-Bragg model that was originally designed to describe helix coil transition in peptides fits properly to experimental data of adsorption of dyes (DY54 and DB22) onto biopolymers (alginic acid and xanthan). The binding of dye molecules to water soluble polymers can take place either by electrostatic interaction between charged groups or by other interactions leading to the formation of polymer-dye complexes. Hydrophobic interactions result in dye and dye-polymer micelle-like hydrophobes in water.

The concordance between the experimental data and theoretical predictions within the Zimm-Bragg model is due to the consideration by Satake and Yang that the interaction between surfactant-biopolymer occurs by two processes, nucleation and aggregation (considered in the Ku and U parameters). In the polymer surfactant systems, the hydrodynamic properties of the biopolymer favors the formation of micelles decreasing de CMC (critical micellar concentration) of the surfactant, thus favoring interaction polymer-surfactant.

In our systems (polysaccharide-dye) we determined the Ku and U values for ALG-DY54 and XANT-DY54 systems with DY54 in commercial and purified form. Interestingly in both cases Zimm-Bragg model describes the interactions. These findings suggest that the dye molecules tend to form aggregates that have similar behavior to that observed with biopolymer-surfactant systems and these aggregates favor the interaction with the alginic acid and xanthan molecules, mainly through hydrogen bonding, electrostatic and hidrofobic interactions. For DY22 this behavior is observed even in the presence of cationic, anionic and neutral surfactants due to the strong tendency of the dye to form aggregates.

Currently, we are working with some other biopolymers, such as pectin and polygalacturonic acid in order to expand our understanding of the nature of interactions involved in the removal of dyes by biopolymers.

5. References

Abbot, L.C.; Batchelor, S.N.; Oakes, J.; Lindsay-Smith, J.R.; Moore, J.N. (2004) Spectroscopic Studies of the Intermolecular Interactions of A Bis-Azo Dye, Direct Blue 1, on Di- and Trimerization in Aqueous Solution and in Cellulose, *J. Phys. Chem. B*, 108, 36, (September 2004) pp. 13726-13735, ISSN: 1520-6106.

Alí, M.F. (2005) Dyes: Chemistry and applications. In *Handbook of Industrial Chemistry, Organic Chemicals*. Alí, M. F.; El-Alí, B.M.; Speight, J.G. Editors 259-288. McGraw-Hill, ISBN- 0-07-141037-6, USA.

Baughman, G. L. and Weber, E. J. (1994) Transformation of Dyes and Related Compounds in Anoxic Sediment: Kinetics and Products *Environ. Sci. Technol.*, 28, 2, (February1994), pp. 267-276, ISSN: 1520-5851

Berlepsch, H. V., Bottcher, C y Dohne, L. (2000) Structure of J aggregates of Pseudoisocyanine dye in aqueous solution *J Phys chem* B, 104, 37, (September 2000), pp. 8792-8799, ISSN: 0021-9606.

Bielska, M.; Sobczynska, A.; Prochaska, K. (2009) Dye-Surfactant Interaction in aqueous solutions. *Dyes and pigments* 80, 2 (February 2009), pp. 202-205, ISSN: 0143-7208.

Blackburn, R.S. (2004) Natural Polysaccharides and Their Interactions with Dyes Molecules: Applications in Effluente Treatment *Environ. Sci. Technol.* 38, 24, (December 2004), pp. 4905-4909, ISSN: 1520-5851.

Chakraborty, S.; Basu, J.K.; De, S.; Dasgupta, S. (2006) Adsorption of Reactive Dyes from a Textile Effluent Using Sawdust as the Adsorbent. *Ind. Eng. Chem. Res.* 45, 13, (June 2006), pp. 4731-4741, ISSN: 0088-5885.

Choy, K.K.H.; Porter, J.F.; McKay, G. (2000) Langmuir Isotherm Models Applied to the Multicomponent Sorption of Acids from Effluent onto Activated Carbon. *J. Chem. Eng. Data* 45,4, (July 2000), pp. 575-584, ISSN: 1520-5134.

Choy, K.K.H.; Porter, J.F.; McKay, G. (2004) Single and Multicomponent Equilibrium Studies for the adsorption of Acidic Dyes on Carbon from Effluents. *Langmuir* 20,22, (October 2004), pp. 9646-9656 ISSN: 0743-7463.

Donati, I., Holtan,S., Morch, Y.A., Borgogna, M., Dentini, M. y Skjak-Braek, G. (2005) New Hypothesis on the Role of Alternating Sequences in Calcium-Alginate Gels. *Biomacromolecules* 6, 2, (March 2005), pp. 1031-1040, ISSN: 1526-4602.

Ferus-Camelo, M.; Greaves, A.J. (2002) An investigation intro Direct Dye Agreggation *Color. Technol.* 118, 1, (January 2002), pp. 15-19, ISSN: 1478-4408

Fugetsu, B.; Satoh, S.; Shiba, T.; Mizutani, T.C; Lin, Y.B.; Terui, N.; Nodasaka, Y.; Sasa, K.; Shindoh, M.; Shibata, K.; Mori, M.; Tanaka, K.; Sato, Y.; Tohji, K.; Tanaka, S.; Nishi, N.; Watari, F. (2004) Caged Multiealled Carbon Nanotubes as the Adsorbents for affinity-Based Elimination of Ionic Dyes. *Environ. Sci. Technol.* 38, 24, (December 2004), pp. 6890-6896, ISSN: 1520-5134.

Freundlich, H.M.F. (1906) Ueber die adsorption in Ioezungen *Z. Phys. Chem.* 57, (February 1906), pp. 385-471, ISSN: 0044-3336

Glazer, N. A. and Nikaido, H. (1995) Microbal Biotechnology, *Fundamentals of Applied Microbiology* W.H. Freeman and Company, second edition, ISBN: 978-0-521-84210-5. USA.

Goodall, D.M. and Norton, I.T. (1987) Polysaccharide conformations and kinetics, *Acc. Chem. Res.* 20, 2, (February 1987), pp. 59-65. ISSN: 0001-4842

Grant, G.T., Morris, E.R., Rees, D.A., Smith, P.J.C.; Thom, D. (1973) Biological Interaction Between Polysaccharides and Divalent Cations: The Egg Box Model *FEBS Lett.* 32, (January 1973), pp. 195-199, ISSN: 0014-5793.

Gibbs, G.; Tobin, J.M.; Guibal, E. (2004) Influence of Chitosan Preprotonation on Reactive Black 5 sorption Isotherms and Kinetics. *Ind. Eng. Chem. Res.* 43, 1, (January 2004), pp. 1-11, ISSN: 0088-5885.

Guzel, B.; Akgerman, A. (1999) Solubility of Disperse and Mordant Dyes in Supercritical CO_2, *J. Chem. Eng. Data,* 44, 1, (December 1999), pp. 83-85, ISSN: 1520-5134.

Hamada, K., Mitshuishi, M., Ohira, M., Miyazaki, K. (1993) Positional effects of Trifluoromethyl Group on the aggregation of Azo Dyes In Aqueous Solutions *J. Phys Chem* 97,19, (May 1993), pp. 4926, ISSN: 0021-9606.

Holme, I. (2000) *Coloration of Technical Textiles*, in: *Handbook of Technical Textiles*; Horrocks, A. R.; Anand, S.C., Editors. 187-222. Woddhead Publishing, ISBN: 1 855733854, Cambridge, U.K.

Hou, A. and Dai, J. (2005) Kinetics of dyeing of polyester with CI Disperse Blue 79 in supercritical carbon dioxide. *Color. Technol.*, 121, 1 (January 2005), pp. 18-20 ISSN: 1472-3581.

Hu, Z.G.; Zhang, J.; Chan, W.L.; Szeto, Y.S. (2006) The Sorption of Acid Dye on to chitosan nanoparticles. *Polymer*, 47, 16, (July 2006), 5838-5842, ISSN: 0032-3861

Karukstis, K.K.; Perelman, L.A.; Wong, W.K. (2002) Spectroscopic Characterization of Azo Dyes Aggregation on Dendrimer Surfaces, *Langmuir,* 18, 26, (December 2002), pp. 10363-10371, ISSN: 0743-7463.

Knapp, J.S. and Newby, P.S. (1995) The microbiological Decolorization o fan Industrial Effluent Containing a Diazo-linked Chromophore. *Water Res*. 29, 7, (July 1995), pp. 1807-1809, ISSN: 0043-1354.

Kromhout, R.A.; Linder, B. (2001) Prediction of Conformational Enthalpy and Heat Capacity from the Zimm Bragg-Theory. *J. Phys. Chem. B* 105, 21, (May 2001), pp. 4987-4991 ISSN: 1520-6106.

Lai, W.C., Dixit, N.S y Mackay, R. A. (1984) Formation of H aggregates of Thionine Dye in Water *J. Phys Chem.* 88, 22, (October 1984), pp. 5364-5368, ISSN: 0021-9606.

Langmuir, I. (1916) The Constitution and Fundamental Properties of Solids and Liquids *J. Am. Chem. Soc*. 38, 11, (November 1916), pp. 2221-2295, ISSN: 0002-7863.

Lee, D.W., Choi, W.S., Byun, M.W., Park, H.J., Yu, Y.M. y Lee, M. C. (2003) Effect of Gama Irradiation on Degradation of Alginate *J. Agric. Food. Chem*. 51, 16, (July 2003), pp. 4819-4823, ISSN 0021-8561.

Lee, J.W.; Min, J.M.; Bae, H.K. (1999) Solubility Measurement of Disperse Dyes in Superciritical Carbon Dioxide *J. Chem. Eng. Data*, 44, 4, (July 1999), pp. 684-687, ISSN: 1520-5134.

Liu, J. ; Takisawa, N. ; Shirahama, K. ; Abe, H.; Sakamoto, K. (1997) Effect of Polymer Size on the Polyelectrolyte-Surfactant Interaction. *J. Phys. Chem. B* 101, 38, (September 1997), pp. 7520-7523 ISSN: 1520-6106.

Lozano-Alvarez, J.A.; Jauregui-Rincon, J.; Mendoza-Diaz, G.; Rodriguez-Vazquez, R. Claudio Frausto-Reyes. (2009 b) Study of Sorption equilibrium of Biopolymers Alginic Acid and Xanthan with C.I. Disperse Yellow 54. *J. Mex. Chem Soc.* 53, 2, (April-June 2009), pp. 59-70 ISSN: 1665-9686.

Maurstad, G.; Danielsen, S.; Stokke, B.T. (2003) Analysis of Compacted Semiflexible Polyaniona Visualizad by Atomic Force Microscopy: Influence of Chain Stiffness on The Morphologies of Polyelectrolyte Complexes. *J. Phys chem.* 107, 40, (october 2003), pp. 8172-8180 ISSN: 0021-9606.

McKay, G.; Blair, H.S.; Gardner, J.R. Adsorption of Dyes on Chitin.I. (1982) Equilibrium Studies. J. Applied Poly Sci. 27, 8, (August 1982), pp. 3043-3057, ISSN: 0021-8995

McKay, G., Wong, Y.C., Szeto, Y.S. y Cheung, W.H. (2003) Equilibrium Studies For Acid Dye Adsorption onto Chitosan *Langmuir* 19, 19, (September 2003), pp. 7888-7894, ISSN: 0743-7463.

Mittal, A. K. and Venkobachar, C. (1996) Uptake of cationic Dyes by Sulfonated Coal: Sorption Mechanism. *Ind. Eng. Chem. Res.* 35, 4, (April 1996), pp. 1472-1474, ISSN: 0088-5885.

Monahan, A. R., Germano, N.J., Blossey, D.F. (1970) Aggregation of Arylazonaphtols.I. Dimerization of Bonadure Red in aqueous and Methanolic systems *J. Phys Chem.* 74, 23, (November 1970), pp. 4014, ISSN: 0021-9606.

Monahan, A. R., Blossey, D.F. (1971) Aggregation of Arylazonaphtols.II.Steric effects on Dimers Structure *J. Phys Chem.* 75, 9, (April 1971), pp. 1227-1233 ISSN: 0021-9606.

Nasr, M.F., El-Ola,S.M.A.,Ramadan,A. y Hazme,A. (2006) A Comparative Studie Between the Adsorption Behavior of Activated Carbon fiber and Modified Alginate I. Basic dyes. *Polymer-Plastics Technology and Engineering* 45, 3, (March 2006), pp. 335-340, ISSN: 1525-6111

Oakes, J.; Dixon, S. (2003) Adsorption of dyes to cotton and inhibition by surfactants, polymers and surfactant-polymer mixtures. *Color. Technol*. 119, 6, (November 2003), pp. 315-323, ISSN: 1472-3581.

Ogawa, T. and Yatome, C. (1990) Biodegradation of Azo Dyes in Multistage Rotating Biological Contractor Inmobilized by assimilating Bacteria. *Bull. Environ. Cont. Toxicol*. 44, 4, (April 1990), pp. 561-566. ISSN: 1432-0800

Özcan, A.S.; Clifford, A.A.; Bartle, K.D. (1997) Solubility of Disperse Dyes in Supercritical Carbon Dioxide *J. Chem. Eng. Data*, 42, 3, (May 1997), pp. 590-592, ISSN: 1520-5134

Poots, V.J.P. and McKay, J.J. (1976) The Removal of Acid dye from Effluent Using Natural Adsorbents-II Wood. *Water Res.* 10, 12, (December 1976), pp. 1067-1070, ISSN: 0043-1354

Reeves, R.L., Maggio,M.S., Harkaway, S.A. (1979) A critical spectrophoptometric analysis of the Dimerization of some ionic Azo Dyes in Ionic solution *J. Phys Chem* 83, 18, (September 1979), pp. 2359-2368, ISSN: 0021-9606.

Rinaudo, M. (2004) Role of sustituents on the properties of some polysaccharides, *Biomacromolecules* 5, 4, (July 2004), pp.1155-1165, ISSN: 1526-4602.

Rodd, A.B., Cooper-White, J.J., Dunstan, D.E. y Boger, D.V. (2001 a) Gel Point studies for chemically modified biopolymer netwoeks using small amplitude scillatory rheometry *Polymer* 42, 1, (January 2001), pp. 185-198, ISSN: 1097-0126.

Rodd, A.B., Cooper-White, J.J., Dunstan, D.E. y Boger, D.V. (2001 b) Polymer Concentration dependence of the Gel point for Chemically Modified Biopolymer Networks Using Small Amplitude Oscillatory Rheometry *Polymer*, 42, 3, (February 2001), pp. 3923-3928, ISSN: 1097-0126.

Satake, I.; Yang, J. T. (1976) Interaction of Sodium Decyl Sulfate with Poly(L-ornithine) and Poly(L-lysine) in Aqueous Solution *Biopolymers* 15, 11, (November 1976), pp. 2263-2275, ISSN: 0006-3525.

Shinoda, T.; Tamura, K. Solubilities of C.I. (2003) Disperse Orange 25 and C.I. Disperse Blue 354 in Supercritical Carbon Dioxide. *J. Chem. Eng. Data* 48, 4, (July 2003), pp. 869-873. ISSB: 1520-5134.

Siew, C. K. and Williams, P.A. (2005) New Insights Into Mechanism of Gelation of Alginate and Pectin: Charge Annihilation and Reversal Mechanism *Biomacromolecules* 6, 2, (March 2005), pp. 963-969, ISSN: 1526-4602

Sun, G.; Xu, X. (1997) Sunflower Stalks as Adsorbents for Color Removal from Textile Wastewater. *Ind. Eng. Chem. Res.* 36, 3, (March 1997), pp. 808-812 ISSN: 0088-5885.

Sung, H.D.; Shim, J.J. (1999) Solubility of C.I. Disperse Red 60 and C.I. Disperse Blue 60 in Supercritical Carbon Dioxide J. Chem. Eng. Data. 44, 5, (September 1999), pp. 985-989 ISSN: 1520-5134.

Tiddy, G. J. T., Mateer, D.L. Ormedrod, A.P., Harrison, W.J., Edwuards, D.J. (1995) Highly Ordered aggregates In Dilute Dye-Water Systems *Langmuir* 11, 2, (February 1995), pp. 390-393, ISSN: 0743-7463.

Torres, E., Mata, Y.N., Blázquez, M.L., Muñoz, J.A., González, F. y Ballester, A. (2005) Gold and Silver Uptake and nanoprecipitation on Calcium Alginate Beads *Langmuir* 21, 17, (August 2005), pp. 7951-7958, ISSN: 0743-7463.

Trung, T.S.; Ng, C.H.; Stevens, W.F. (2003) Characterization of Decrystallized chtitosan and its application in biosorption of Textile dyes. *Biotechnology Letters* 25, (July 2003), pp. 1185-1190 ISSN: 0141-5492.

Wong, Y.C.; Szeto, Y.S.;, Cheung, W.H.; McKay, G.M. (2004) Adsorption of Acid Dyes on Chitosan-equilibrium Isotherms analyses. *Process Biochem.* 39, 6, (February 2004), pp. 695-704, ISSN: 1359-5113.

Zimm, B.H. and Bragg, J.K. (1959) Theory of Phase Transition Between Helix and Random Coil in Polypeptide Chains *J. Chem. Phys.* 31, 2, (August, 1959), pp. 526-535, ISSN: 0021-9606.

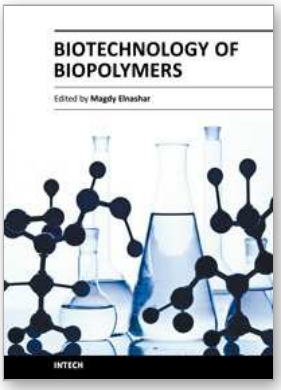

Biotechnology of Biopolymers

Edited by Prof. Magdy Elnashar

ISBN 978-953-307-179-4
Hard cover, 364 pages
Publisher InTech
Published online 24, June, 2011
Published in print edition June, 2011

The book "Biotechnology of Biopolymers" comprises 17 chapters covering occurrence, synthesis, isolation and production, properties and applications, biodegradation and modification, the relevant analysis methods to reveal the structures and properties of biopolymers and a special section on the theoretical, experimental and mathematical models of biopolymers. This book will hopefully be supportive to many scientists, physicians, pharmaceutics, engineers and other experts in a wide variety of different disciplines, in academia and in industry. It may not only support research and development but may be also suitable for teaching. Publishing of this book was achieved by choosing authors of the individual chapters for their recognized expertise and for their excellent contributions to the various fields of research.

INTECH
open science | open minds

InTech Europe
University Campus STeP Ri
Slavka Krautzeka 83/A
51000 Rijeka, Croatia
Phone: +385 (51) 770 447
Fax: +385 (51) 686 166
www.intechopen.com

InTech China
Unit 405, Office Block, Hotel Equatorial Shanghai
No.65, Yan An Road (West), Shanghai, 200040, China
中国上海市延安西路65号上海国际贵都大饭店办公楼405单元
Phone: +86-21-62489820
Fax: +86-21-62489821